The Experimental Determination of Velocity Distribution in Annular Flow

D. A. Simmers† and J. E. R. Coney‡

In the study of the flow of a fluid through an annular gap, the outer surface of which is stationary while the inner surface may be rotated, it is necessary to be able to accurately determine the velocity profiles obtaining in the axial, tangential, and radial directions of flow.

A method is described for this purpose employing hot-wire anemometry techniques and typical profiles are presented for each of the above flow directions. In the case of pure axial flow, a comparison is made between experimental and theoretical results, showing a close correspondence.

NOTATION

A	a constant
b	annular gap width $(R_2 - R_1)$
B	a constant
d_e	equivalent diameter of annulus $\{2(R_2 - R_1)\}$
k_1	yaw factor
k_2	pitch factor
n	a constant
N	annular radius ratio (R_1/R_2)
R	general radial co-ordinate
R_1	radius of inner annular surface
R_2	radius of outer annular surface
R'	dimensionless radial gap position $(R_2 - R)/(R_2 - R_1)$
Re_a	axial Reynolds number $\{(u_a)_{av} d_e/\nu\}$
Ta	Taylor number, $2\Omega_1^2 R_1^2 b^3/\nu^2(R_1 + R_2)$ (wide gap case)
u	velocity component
U	general velocity
U_{eff}	effective cooling velocity
V	voltage
α	yaw angle
ν	kinematic viscosity of fluid
θ	pitch angle
Ω_1	angular velocity of inner annular surface

Subscripts

a	axial flow direction
at	resultant of a and t
av	average value
r	radial flow direction
t	tangential flow direction

1 INTRODUCTION

In their development of a Reynolds analogy-type solution for the heat transfer characteristics of combined axial and Taylor vortex flows, the authors (**1**) required a knowledge of the distributions of the velocities prevailing in these flows. However, such information was found to be available only for Taylor vortex flow with zero imposed axial flow. Bjorklund and Kays (**2**) in their analogy solution for the heat transfer characteristics of Taylor vortex flow had used the data of Pai (**3**) to formulate the required nondimensional velocity distribution, but the authors found that these results differed from those of Taylor (**4**). Since the effects of a superimposed axial velocity were unknown, and the results of the only two investigations available (**3**, **4**) differed markedly, it was considered essential to investigate the velocity distribution of combined Taylor vortex and axial flows, the accuracy of the proposed analogy depending on that of the velocity data used in its formulation.

Taylor (**4**) investigated the circumferential velocity distribution of Taylor vortex flow, using water as the working fluid, by consideration of the pressure difference between the pressure in a small Pitot tube and that in a small hole in the outer cylinder. Using a Pitot tube of 0·48 mm diameter, he found that this pressure difference varied radially from a high value close to the rotating inner boundary, through a minimum at about one-third of the gap width, to a maximum at about nine-tenths of the gap width from which there was a rapid fall to zero at the stationary outer boundary. Using a larger Pitot tube (1·12 mm diameter), he observed the same effect but with an accentuation of the difference between the maximum and minimum values of the pressure difference. He concluded that the differences in the two sets of measurements were due to the protrusion of the Pitot tube into the flow; in the case of zero axial flow, the wake thus produced is carried round circumferentially by the fluid and forms a ring-shaped region where the velocity differs from that which would exist in the absence of the Pitot tube. Using data from the two Pitot tubes, and, assuming that the velocity deficiency in the wake was proportional to the resistance of the obstruction, he evaluated the true distribution of the pressure difference by extrapolation to zero Pitot size. From these corrected results, he showed that the pressure difference (and hence $u_t R$) remained constant across 83 per cent of the annular gap width. Thus Taylor found the tangential velocity distribution in Taylor vortex flow to be characterized by two regions of high velocity gradient, close to the annular boundaries, surrounding a central region, occupying about 83 per cent of the gap width, in which the velocity gradient was smaller.

Pai (**3**) investigated the circumferential velocity distribution of Taylor vortex flow, using air as the working fluid, by means of hot-wire anemometry. Measurements of mean velocity and of the root mean square of the

† UKAEA, Risley, Warrington WA3 6AT.
‡ Department of Mechanical Engineering, University of Leeds, Leeds LS2 9JT.

Received 14 May 1979 and accepted for publication on 24 August 1979.

0142/727X/79/1200-0177$02.00

velocity fluctuations indicated that two types of flow existed, depending on the position of the probe relative to the vortex cells. Both types of flow exhibited a constant value of mean velocity, equal to half of the velocity of the rotor surface, across the central 60 per cent of the gap. The two types of flow were characterized by differing velocity distributions close to the annular boundaries, which were attributed to the vortices assuming an ellipsoidal form, separated by regions of turbulence.

Although Pai (3) realized that the vortices constituted a three-dimensional velocity field, he overlooked the effect of the radial and axial velocity components on the measurements of the hot-wire probe. It may be gathered from reference (3) that the probe was oriented such that the sensing wire was perpendicular to the tangential velocity, in which position the axial and radial components of velocity have a small, but significant, effect. The method of Taylor (4) would not be affected by such considerations since the Pitot tube is sensitive mainly to velocities flowing along the axis of the tube.

Thus the results of references (3) and (4) yielded different conclusions as to the tangential velocity distribution in Taylor vortex flow, the differences possibly being due to the neglect of the effects of the three-dimensional velocity field on the part of Pai (3).

From the information given in these papers, the Taylor numbers, for which results were presented, have been assessed by the authors as $6{\cdot}97 \times 10^7$ and $1{\cdot}056 \times 10^{10}$ for the data of (3) and (4), respectively. Thus a further possible explanation for the observed differences is that the two workers were investigating different flow regimes; at the lower value of Taylor number studied by Pai (3), the vortices still retain the solid body rotation associated with the simple toroidal form of vortex observed at initial onset, whereas under the conditions considered by Taylor, the vortices exist but are very complex and no longer retain solid body rotation resulting in a velocity gradient across the vortex core.

It was against this uncertain background that the present study was initiated. With the improved anenometry techniques available to them, the authors considered it possible to obtain accurate distributions for at least two of the three velocity components obtaining in combined Taylor vortex and axial flows.

2 DIRECTIONAL CHARACTERISTICS OF HOT-WIRE PROBES

In most anemometry applications, a proper interpretation of the anemometer output signals requires that the directional sensitivity of the wire should be known. In the present application, it was required that all three components of the velocity field, should be obtained from signals from a single probe. Jorgenson (5) has shown that yaw and pitch are important when a hot-wire probe is placed in a three-dimensional velocity field. In Fig. 1, such a probe is shown subjected to a general velocity, U, composed of the three components for annular flow with inner cylinder rotation, u_r, u_a, and u_t acting in the radial, axial, and tangential direction, respectively; the sensing wire is shown in the a-plane and the probe axis in the r-plane. The probe is normally calibrated in the position where $\alpha = \theta = 0°$, i.e., in the direction of the r-axis. Considering a velocity of unit magnitude flowing along the r-axis, this velocity will be registered as being

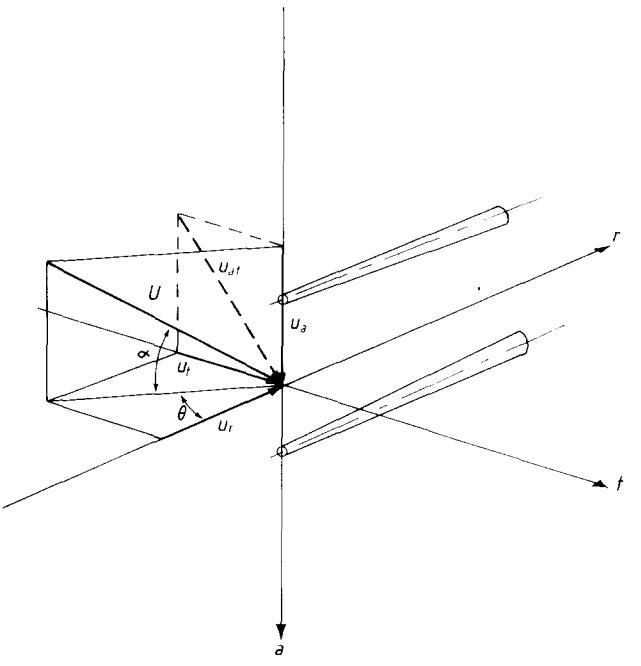

Fig. 1. A hot-wire probe subjected to a three-dimensional velocity field in an annular gap with inner cylinder rotation

of unit magnitude since the calibration was obtained in this position. If this unit velocity is now allowed to rotate in the a-r plane from $\alpha = 0°$ to 90°, the cooling effect of that velocity will decrease with increasing angle. Accordingly, a velocity of unit magnitude flowing along the a-axis will have a smaller effect than that which would result from flow along the r-axis, and consequently, the velocity, as registered by the anemometer, would be less than that actually obtaining. For this reason a yaw factor, k_1, has to be included as a correcting factor for the tangential cooling velocity. A similar, although less obvious, situation occurs if the velocity is rotated in the r-t plane from $\theta = 0°$ to 90°, and for this reason a second factor, k_2, the pitch factor, is required to correct for velocity vectors out of the sensor-prong planes.

Referring to Fig. 1, and using the two factors, k_1 and k_2, the effective cooling velocity acting on the sensor can be expressed as

$$U_{\text{eff}}^2 = u_r^2 + k_1^2 u_a^2 + k_2^2 u_t^2 \tag{1}$$

and, it can be seen from Fig. 1, that

$$U_{\text{eff}}^2(\alpha) = U(0)^2(\cos^2 \alpha + k_1^2 \sin^2 \alpha) \qquad \text{for } \theta = 0° \tag{2}$$

$$U_{\text{eff}}^2(\theta) = U(0)^2(\cos^2 \theta + k_2^2 \sin^2 \theta) \qquad \text{for } \alpha = 0° \tag{3}$$

where $U_{\text{eff}}(\alpha)$ and $U_{\text{eff}}(\theta)$ are the effective cooling velocities at angles α and θ, respectively, and $U(0)$ is the velocity in the direction of $\alpha = 0°$ or $\theta = 0°$. For a probe with a calibration equation given by

$$V^2 = A + BU^n \tag{4}$$

eqs. (2)–(4) yield

$$k_1 = \frac{1}{\sin \alpha} \left| \frac{|V(\alpha)^2 - A|^{2/n}}{|V(0)^2 - A|} - \cos^2 \alpha \right|^{1/2} \tag{5}$$

$$k_2 = \frac{1}{\sin \theta} \left| \frac{|V(\theta)^2 - A|^{2/n}}{|V(0)^2 - A|} - \cos^2 \theta \right|^{1/2} \tag{6}$$

where $V(\alpha)$, $V(\theta)$, and $V(0)$ represent the anemometer output voltages measured at angles, α, θ, and 0°, respectively.

To check the directional characteristics of the probes used in the present study, a number of calibrations were effected on the DISA calibration apparatus (DISA units 55D44, 45, 46) which has a built in facility for variation of both pitch and yaw angles. Calibrations were performed under two conditions with ($\theta = 0°$, $0° \leqslant \alpha \leqslant 90°$) and ($\alpha = 0°$, $0° \leqslant \theta \leqslant 90°$) to obtain the variation of the yaw and pitch factors, k_1 and k_2, with variation in α and θ, respectively. Double wire probes, type 55P71, purchased to provide temperature compensation in diabatic studies were used for this purpose. However, for the present study, only one wire was required to act as a velocity sensor, care being taken to ensure that the velocity sensor was always upstream of the second wire, to preclude any effects of flow interference resulting from the second wire. The probe was connected to a DISA CTA standard bridge, type 55M10, housed in a DISA 55M01 main unit, and the probe output voltage was monitored by a DISA digital voltmeter, type 55D30.

A typical set of results for the angular variation of k_1 and k_2, calculated from eqs. (5) and (6) is shown in Fig. 2 for three velocities. In Fig. 2(a), k_1 is seen to decrease with increasing yaw angle, α, indicating that a given velocity has a decreasing effect on the sensor as α increases. The effect of velocity on k_1 appears to be random but it may be seen that the spread of the results is worse at small values of α. Figure 2(b) shows that k_2 is virtually constant for all values of θ, but again the spread of the results is worse at low values of θ. The value of k_2 is greater than unity indicating that a velocity striking the probe from a direction outside the sensor-prong plane has a larger effect on the sensor, than if that same velocity were flowing along the r-axis.

This exercise was repeated for several probes and it was found that, although the probes were of the same type, the values of k_1 and k_2 could vary considerably from one probe to another. However, the trends of Fig. 2 were always maintained.

3 EXPERIMENTAL TECHNIQUE

To enable the separation of the three velocity components, three simplifications were made to the generalized treatment of the preceding section. The first of these may be understood by reference to Fig. 1, this simplification deriving from the resolution of the general velocity vector, U, into two components rather than three. Instead of resolving the general velocity into the axial, tangential, and radial components, u_a, u_t, and u_r the latter component, u_r is retained and the axial and tangential components are combined to form a resultant velocity, u_α, shown by the broken line.

The second simplification derives from the linearization of the output signal by means of a DISA linearizer, type 55D10, interposed between the anemometer bridge and the digital voltmeter. Thus the calibration of the probe assumes the form

$$V^2 = A + BU^2 \tag{7}$$

and, in all instances, the calibration was effected such that $A = 0$ and $B = 1$, i.e., the calibration equation becomes $V = U$. The use of the linearized output considerably simplifies the calculation of results.

In Fig. 1, it may be seen that the probe enters the velocity field along the radial axis, r, while being free to rotate about that axis. However, rotation of the probe will yield no information regarding the angles α and θ and the third simplification is made to overcome this deficiency. Figure 2(b) shows that the pitch factor, k_2, is almost invariant with θ, and hence the magnitude of θ need not be known. Figure 2(a), shows that the yaw factor, k_1, varies with α, and the lack of information regarding α could lead to error in the determination of velocity. Jorgenson (5) presented results for the relative error in velocity as a function of α, which would result if the yaw factor were considered constant at the values

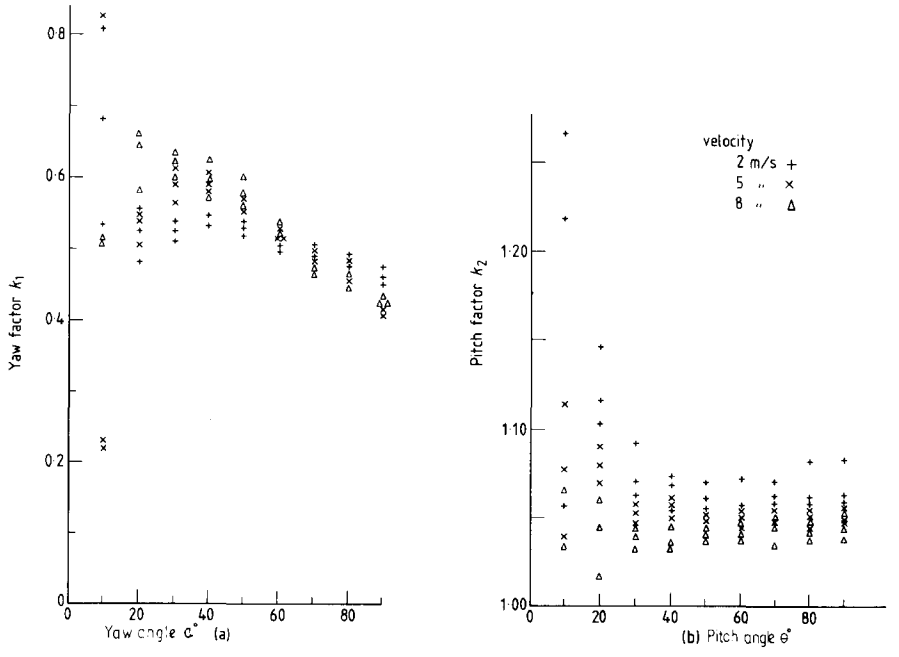

Fig. 2. Yaw and pitch factor versus yaw and pitch angle for nonlinearized anemometer. (a) yaw angle $\alpha°$. (b) pitch angle $\theta°$

$k_1(0)$, $k_1(60)$, and $k_1(90)$, i.e., the values of k_1 calculated from eq. (5) with $\alpha = 0°$, 60°, and 90°, respectively. These results indicated that the relative error was large for $k_1(0)$, reaching a maximum error of 50 per cent at $\alpha = 90°$, whereas for $k_1(90)$ the lowest errors resulted, with a maximum relative error of 10 per cent at $\alpha = 75°$. These conclusions, taken with the fact that the values of k_1 and k_2, presented in Fig. 2, were more repeatable at high values of α and θ, led to the use of $k_1(90)$ and $k_2(90)$ in the present investigation, where $k_1(90)$ is the yaw factor for $\alpha = 90°$, and $k_2(90)$ is the pitch factor for $\theta = 90°$.

From Fig. 1, it is clear that rotation of the probe will have no effect on the cooling influence of the radial velocity, u_r. However, the probe output voltage will alter as the probe is rotated because of the changing orientation of the resultant, u_{at}. The minimum voltage will be registered when u_{at} is in line with the sensing wire, i.e., on the a-axis, the a and t axes rotating with the probe. In this position, the effective cooling velocity is given by

$$U_{\text{eff}}^2 = u_r^2 + k_1^2(90)u_{at}^2 \tag{8}$$

From eqs. (7) and (8) with $A = 0$ and $B = 1$, it may be shown that

$$V_{\text{min}}^2 = u_r^2 + k_1^2(90)u_{at}^2 \tag{9}$$

If the probe is now rotated through 90° (and the a and t axes with it) a maximum voltage is registered since the resultant, u_{at}, is now along the t-axis which is perpendicular to the sensing wire. The effective cooling velocity in this position is given by

$$U_{\text{eff}}^2 = u_r^2 + k_2^2(90)u_{at}^2 \tag{10}$$

which for a linearized anemometer with $V = U$, can be rewritten as

$$V_{\text{max}}^2 = u_r^2 + k_2^2(90)u_{at}^2 \tag{11}$$

Thus, since $k_1(90)$ and $k_2(90)$ are known from calibration, and V_{max} and V_{min} can be found by measurement, eqs. (9) and (11) can be solved for the two unknowns of u_r and u_{at}. In addition, the angular orientation of the probe necessary to achieve a minimum output voltage corresponds to the direction of u_{at}. If this orientation is known with respect to either the axial or tangential directions of the annular gap, the resultant velocity, u_{at}, can be resolved into its constituent components of u_a and u_t the axial and tangential velocities. Thus, the three components of the velocity distribution can be separated from the readings of a single probe taken at two orientations.

Calibration of the probe was effected on the DISA calibration rig in the normal calibration position of $\alpha = \theta = 0°$ such that the linearized anemometer output obeyed the relationship of $V = U$, over the velocity range investigated. Two further calibrations were then obtained under conditions of ($\theta = 0°$, $\alpha = 90°$) and ($\alpha = 0°$, $\theta = 90°$) to yield results for $k_1(90)$ and $k_2(90)$ as functions of velocity; a typical set of linearized results is shown in Fig. 3. The scatter on both of these figures is very small in accordance with the observations of Fig. 2, that the scatter of results decreased markedly as the angles, α and θ, became larger. The dependency of $k_1(90)$ and $k_2(90)$ on velocity indicates that low velocities striking the sensor from outside the calibration direction

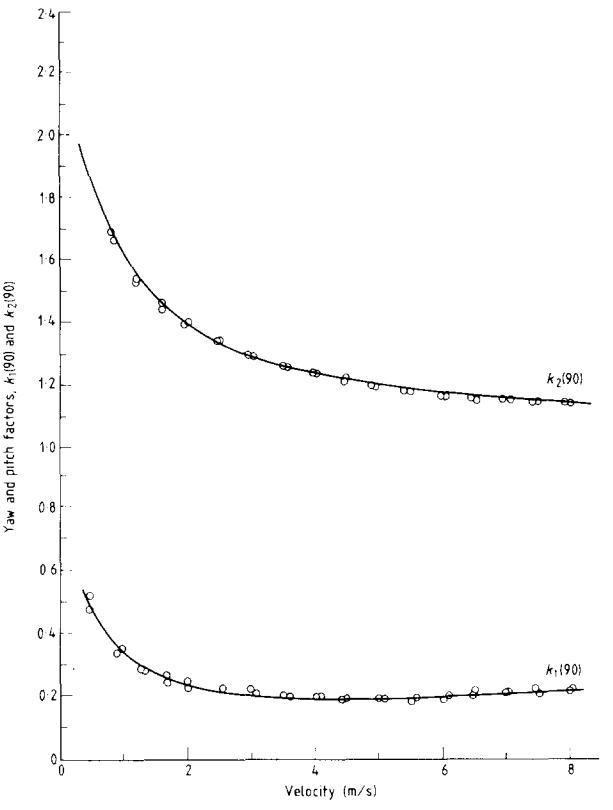

Fig. 3. Variation of yaw and pitch factor with velocity for linearized anemometer

have a much larger effect on the probe, in relation to their effects in the calibrated direction of $\theta = \alpha = 0°$, than do larger velocities. Neglect of this phenomenon could lead to serious errors in the calculated results.

The heat transfer apparatus used in this study is described in essence in (**1**) and more fully in (**6**). It consisted essentially of a vertical concentric annulus through which the working fluid, air, was passed. It comprised a stationary steel tube of inside diameter 139·7 mm and an inner rotatable cylinder of Tufnol. Two such cylinders existed of diameter 133·4 mm and 111·8 mm, giving radius ratios N of 0·955 and 0·8, respectively; the length of these cylinders was 1·82 m. Twenty-nine measuring stations were placed along the annulus so that velocity and temperature measurements could be obtained. The calibrated probe was placed in the annular gap of this apparatus, at an axial position which ensured that the flow would be fully developed under all conditions.

The orientation of the probe was determined with respect to the axial direction of the annular gap by subjecting the probe to a high, laminar axial flow; values of minimum and maximum voltage were found by rotation of the probe about its own axis, and the results of several determinations were averaged to give the angle, corresponding to the axial direction of flow. Throughout this procedure, care was taken that the velocity sensing wire was always upstream of the second wire.

For a constant value of axial Reynolds number, tests were effected at various rotational speeds of the inner cylinder. At each speed, a radial traverse was made over ten equal increments, from the outer wall to a position one tenth of the gap width away from the rotating

surface; in the case of the radius ratio $N = 0{\cdot}8$, a further measurement was taken at one fortieth of the gap width from the rotating surface. At each position, measurements were taken of V_{min}, V_{max} and the angular orientation of the probe. From this information, values of $k_1(90)$ and $k_2(90)$ were determined for each position and the three velocity components calculated. From the measurements of the mass flow and mean temperature of the air in the annular gap and the rotational speed of the inner cylinder, the axial Reynolds numbers and the Taylor numbers were determined also.

The mass rate of flow of the air was determined by means of a range of orifice plates, designed according to British Standards Specification 1042, and positioned well upstream of the apparatus. This flowrate was checked by velocity measurements, made within the annular gap, using a hot-wire probe. The gap was divided into ten equal parts and the resulting velocity profile integrated, the average velocity thus determined being compared with that given by the orifice plate and inclined water manometer. The difference between the two values, taken over a range of axial flows ($Re_a <$ 2500), indicated an average discrepancy of approximately 3 per cent for $Re_a^2/Ta = \infty$. Considering now the accuracy of these measurements when the inner cylinder is rotated, experimental values of $(u_a)_{av}$ obtained for a range of values of Re_a^2/Ta may be compared with a theoretical value. Using the expression for axial Reynolds number given under Notation, a fluid temperature of 25° C, an annular radius ratio of 0·955 and an axial Reynolds number of 400 yield a theoretical average axial velocity of 0·988 m/s. From the integration of velocity profiles, experimental average axial velocities were determined, Fig. 4 showing the variation of the ratio of these experimental values to the theoretical with Re_a^2/Ta.

The rotational speed of the inner cylinder was registered on an Advance Electronics 15 MHz timer/counter, type TG12A, which was fed by a magnetic pick-up, counting off six marks scored on the steel component at the base of the inner cylinder. The counter could be used in two modes giving resolutions of 1 rev/min or 10 rev/min, as required.

The hot-wire probe was traversed radially across the annular gap by a micrometer device, giving an accuracy of ±0·012 mm. The angular position of this probe was determined by a simple protractor giving an accuracy of ±1°. This instrumentation is fully described in (6).

4 PRESENTATION AND DISCUSSION OF RESULTS

Before presenting results of the present study, the physical meaning of these results will be considered. Although the hot-wire probe has a very short response time, the response of the digital voltmeter must be suitably damped to enable measurements to be taken, and consequently the measurement is of mean effects rather than of the fluctuations present in the flow. However, with regard to convective heat transfer, the mean velocity components are more important than the associated velocity fluctuations, and thus, for the purposes for which the velocity profiles were obtained, the determination of mean effects is sufficient.

In Taylor vortex flow with a superimposed axial flow, the axial and tangential velocity components both consist of a mean velocity with superimposed fluctuations. The radial velocity component, however, consists entirely of fluctuations about zero velocity, there being no net motion in the radial direction. Since the hot-wire probe is unable to discriminate between positive and negative velocities, the physical meaning of the results

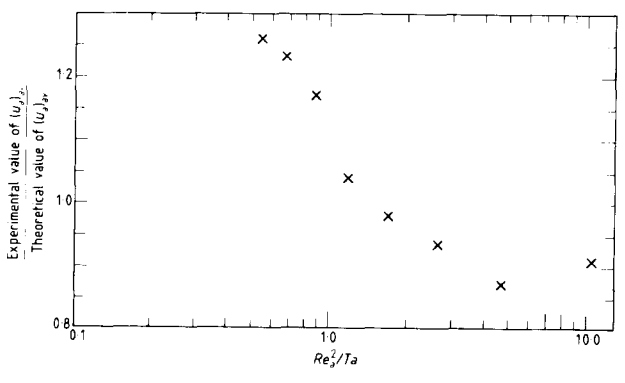

Fig. 4. Variation of (Experimental value of $(u_a)_{av}$)/(Theoretical value of $(u_a)_{av}$) with Re_a^2/Ta

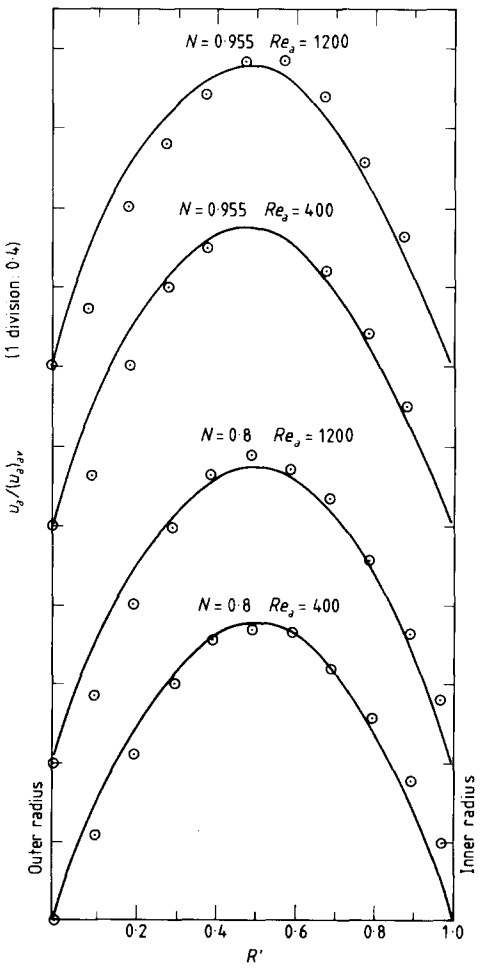

Fig. 5. Comparison of theoretical and experimental adiabatic axial velocity profiles ($Re_a^2/Ta = \infty$). ⊙ Experimental, — Theoretical (7)

obtained for this component must be clarified. In such a case, the probe will sense the root mean square effect of the fluctuations and the results will be a measure of the amplitude of those fluctuations.

Hence, it was considered possible to obtain meaningful results for the axial and tangential velocity distribution in such a flow, but the results of the radial velocity profile would be less clear. An investigation was conducted over the range of axial Reynolds numbers $300 \leqslant Re_a \leqslant 1600$. A small proportion of those results are presented here, for the purpose of illustration.

4.1 Axial Velocity Distribution

The results of axial velocity distribution in adiabatic flow for radius ratios of 0·8 and 0·955 but with zero rotation of the inner cylinder are given in Fig. 5. Figure 6 also shows such distributions but for a radius ratio of 0·955 only and with rotation of the inner cylinder, Re_a^2/Ta being used as a similarity parameter. These figures are carpet plots, the origin of each curve being shifted to separate the sets of points. The velocity was normalized with respect to the average axial velocity obtaining as determined by Simpson's rule, and was plotted against the dimensionless gap position R'.

In Fig. 5, for each set of experimental results, a theoretical profile was calculated from an expression derived from Knudsen and Katz (7)

$$\frac{u_a}{(u_a)_{av}} = \frac{2}{1 + N^2 + \dfrac{1 - N^2}{\ln N}} \times \left\{1 - \left(\frac{R}{R_2}\right)^2 - \frac{(1 - N^2)}{\ln N} \ln\left(\frac{R}{R_2}\right)\right\} \quad (12)$$

It will be noted that there is good agreement between the theoretical and experimental results, although the latter are skewed towards the inner surface, those for $N = 0{\cdot}955$ more so than those for $N = 0{\cdot}8$. Two reasons are offered for this deviation. First, the finite length of the sensing wire could cause measurements in the vicinity of the inner surface to be slightly higher than the required, actual velocity value, owing to the positive velocity gradient obtaining in that region, and vice versa for the case of the outer surface, where there is a negative velocity gradient. This effect was noted by Astill in his discussion on the paper of Sparrow and Lin (**8**), and also by El-Shaarawi (**9**). Secondly, inaccuracies in probe positioning would have a greater effect in the small gap

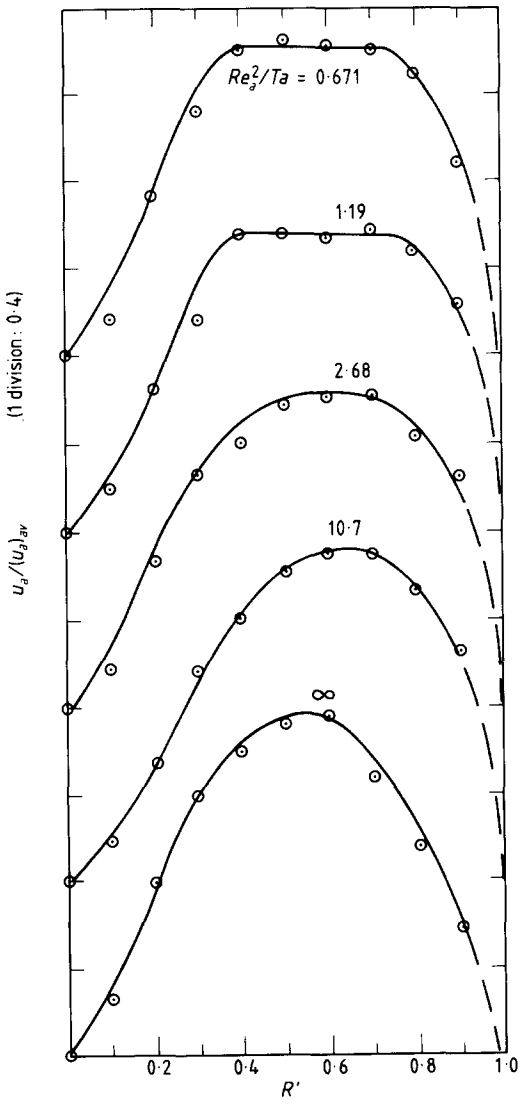

Fig. 6. Adiabatic axial velocity profiles: $N = 0{\cdot}955$, $Re_a = 400$

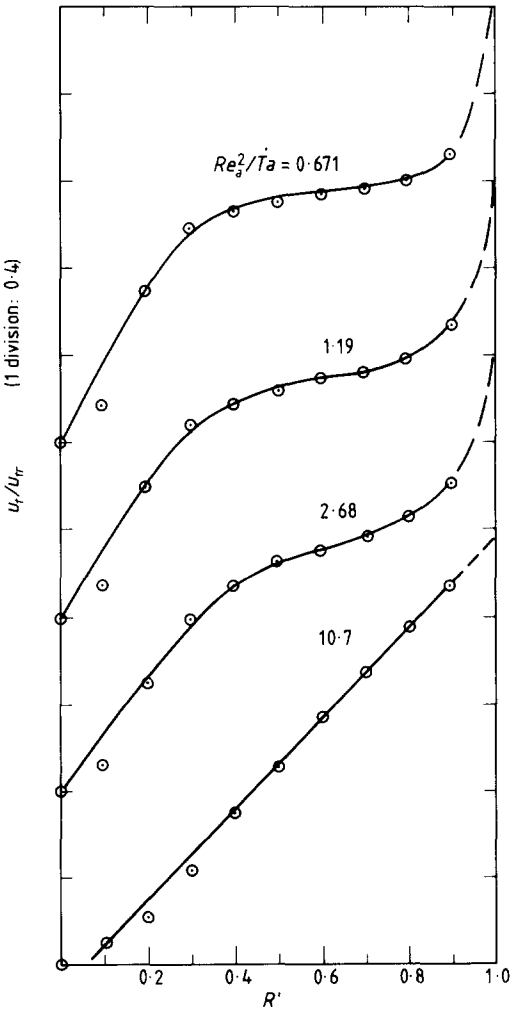

Fig. 7. Adiabatic tangential velocity profiles: $N = 0{\cdot}955$, $Re_a = 400$

width for $b = 3{\cdot}15$ for $N = 0{\cdot}955$; an inaccuracy of 0·1 mm would be highly significant for this case, but would be less important for $N = 0{\cdot}8$, where $b = 12{\cdot}95$ mm.

From Fig. 6 the velocity profile for pure axial flow ($Re_a^2/Ta = \infty$) is seen to be not greatly affected when $Re_a^2/Ta = 10{\cdot}7$, Couette flow still prevailing. However, at values of Re_a^2/Ta lower still, vortex flow has occurred and, as it strengthens, the profile increasingly flattens. This flattened 'core' of the profile and the associated decrease in maximum velocity are consistent with the vortex moving axially as a body.

4.2 Tangential Velocity Distribution

Tangential velocity profiles are presented in Fig. 7 in the form of a 'carpet' plot, the tangential velocity being normalized with respect to the inner cylinder velocity. The plots shown in the figure are for the flow when subcritical ($Re_a^2/Ta = 10{\cdot}7$) and supercritical ($Re_a^2/Ta = 2{\cdot}68$, $1{\cdot}19$, $0{\cdot}671$). The experimental points, in the subcritical case, approximate well to a straight line as would be expected for Couette flow. In the supercritical cases, the distribution, for the Taylor vortex flow existing under these conditions, is shown to be characterized by a central region of relatively small velocity gradient bounded by regions of high velocity gradients close to the boundaries of the annular gap. It will be recalled that in Section 1 it was stated that Taylor (4) had observed this form also.

4.3 Radial Velocity Distributions

The results for radial velocity distribution are presented in Fig. 8; the velocity in this case has not been normalized since there is no reference velocity which can be used for this purpose. It should be remembered that this figure presents results for the distribution of the amplitude of the fluctuating radial component, rather than of the mean velocity component. At $Re_a^2/Ta = 2{\cdot}68$ vortex flow just having occurred, the velocity distribution is seen to be constant across most of the gap width, as might be expected if the vortices retained the form of the simple Taylor vortex. At lower values of Re_a^2/Ta, a dual peak distribution becomes increasingly pronounced, indicating some fundamental change in vortex form.

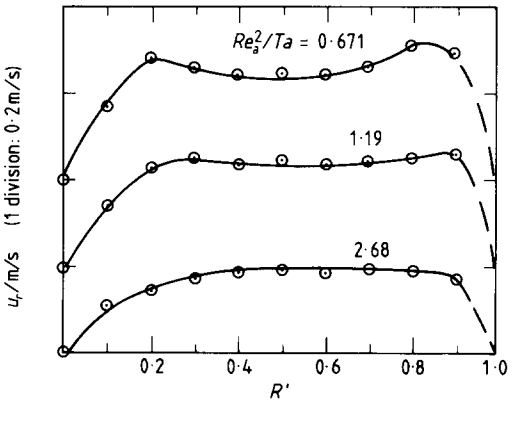

Fig. 8. Adiabatic radial velocity profiles: $N = 0{\cdot}955$, $Re_a = 400$

However, a physical explanation cannot be offered to account for these profiles.

5 CONCLUSIONS

A method has been presented which satisfactorily separates all three velocity components obtaining in the three-dimensional velocity field induced by the presence of Taylor vortex flow, with a superimposed axial flow.

This method will be of value to experimentalists working in the field of annular flow, especially those in engineering research and development concerned with tribology and heat transfer.

APPENDIX

Probe Interference

One of the main problems encountered by Taylor (4), for the case of zero axial flow, was the interference caused by the protrusion of the probe into the flow, as was described in Section 1. This problem was alleviated in the present study by the inclusion of the axial velocity component which carried the wake, produced by the probe, downstream of the probe. However, under conditions of low axial velocity and/or high rotational speed, the wake may not be carried sufficiently far downstream to eliminate all effects on the measurements.

Close to the outer annular surface, low axial and tangential velocities prevail. However, the problem of interference at this position is mitigated by the small protrusion of the probe; the diameter of the sensing wire is 5 μm and the diameter of the tapered support prongs at the tips is about 0·1 mm; these small dimensions offer only minimal interference.

In the middle of the annular gap, the effects of interference can be quantified with regard to the results presented in Section 4. For the worst case of the lowest axial velocity investigated at $Re_a = 300$ and $N = 0{\cdot}8$, and highest inner rotational speed of 1000 rev/min, it was found that $(u_{a,\max})/(u_a)_{av} = 1{\cdot}15$ and $u_t/\Omega_1 R_1 = 0{\cdot}33$ (giving the mid-gap velocity components as $u_a = 0{\cdot}170$ m/s and $u_t = 1{\cdot}95$ m/s). Thus with a sensor wire of length 1·25 mm, supported by prongs with a maximum diameter of 0·5 mm, the width of the wake should be at least 2·25 mm, but, for each revolution of the rotor, the axial movement is found to be 3·06 mm (from the velocity data given above). Thus at mid-gap the effect of the wake produced by the probe should be negligible.

Near to the inner annular boundary, the combination of low axial flow and high tangential velocity causes a significant probe interference effect. Thus measurements taken at $R' = 0{\cdot}9$ will probably give lower values of velocity than those actually obtaining, due to the velocity deficiency of the wake.

Hence, the large velocity gradients observed at the inner annular surfaces in the tangential velocity profiles are probably greater than those actually obtaining, this effect being most pronounced at the lowest values of Re_a^2/Ta investigated. However, since the present study was concerned with obtaining velocity profiles for an analogy solution, which only required the velocity gradients close to the outer wall (that being the heat transfer surface), these errors of measurement close to the inner surface are not important in this case.

REFERENCES

(1) SIMMERS, D. A., and CONEY, J. E. R. 'A Reynolds analogy solution for the heat transfer characteristics of combined Taylor vortex and axial flows', *Int. J. Heat Mass Transfer* 1979, **22**, 679–689

(2) BJORKLUND, I. S., and KAYS, W. M. 'Heat transfer between rotating concentric cylinders', *Trans. Amer. Soc. mech. Engrs. J. Heat Transfer* 1959, **81**, 175–186

(3) PAI, S. I. 'Turbulent flow between rotating cylinders', 1943 *NACA Tech. Note no. 892*

(4) TAYLOR, G. I. 'Distribution of velocity and temperature between concentric rotating cylinders', *Proc. Roy. Soc.* Lond. Series A 1935, **151**, 494–512

(5) JORGENSEN, F. E. 'Directional sensitivity of wire and fibre-film probes', *Disa Information* 1971, **11**, 31–37

(6) SIMMERS, D. A. 'The development, hydrodynamics and heat transfer characteristics of a rotary heat exchanger', *Ph.D. thesis*, Leeds University, UK, 1976

(7) KNUDSEN, I. G., and KATZ, D. L. 'Fluid dynamics and heat transfer', 1958 (McGraw-Hill, New York)

(8) SPARROW, E. M., and LIN, S. H. 'The developing laminar flow and pressure drop in the entrance region of annular ducts', *Trans. Amer. Soc. mech. Engrs. J. Basic Engineering Series D* 1964 **86** (no. 4), 827–834

(9) EL-SHAARAWI, M. A. I. 'Heat transfer and hydrodynamics in the entrance region of concentric annuli with stationary and rotating inner walls', *Ph.D. thesis*, Leeds University, UK, 1974